

1 **Rapid reduction in ecosystem productivity caused by flash drought based on**
2 **decade-long FLUXNET observations**

3 Miao Zhang^{a,c}, Xing Yuan^{b*}

4 ^aKey Laboratory of Regional Climate-Environment for Temperate East Asia
5 (RCE-TEA), Institute of Atmospheric Physics, Chinese Academy of Sciences, Beijing
6 100029, China

7 ^bSchool of Hydrology and Water Resources, Nanjing University of Information
8 Science and Technology, Nanjing 210044, China

9 ^cCollege of Earth and Planetary Sciences, University of Chinese Academy of Sciences,
10 Beijing 100049, China

11

12

13

Submitted May 7, 2020

14

Revised October 19, 2020

*Corresponding author address: Xing Yuan, School of Hydrology and Water Resources, Nanjing University of Information Science and Technology, Nanjing 210044, China E-mail: xyuan@nuist.edu.cn

15 **Abstract.** Flash drought is characterized by its rapid onset and arouses wide concerns
16 due to its devastating impacts on the environment and society without sufficient early
17 warnings. The increasing frequency of soil moisture flash drought in a warming
18 climate highlights the importance of understanding its impact on terrestrial
19 ecosystems. Previous studies investigated the vegetation dynamics during several
20 extreme cases of flash drought, but there is no quantitative assessment on how fast the
21 carbon fluxes respond to flash drought based on decade-long records with different
22 climates and vegetation conditions. Here we identify soil moisture flash drought
23 events by considering decline rate of soil moisture and the drought persistency, and
24 detect the response of ecosystem carbon and water fluxes to soil moisture flash
25 drought during its onset and recovery stages based on observations at 29 FLUXNET
26 stations from croplands to forests. Corresponding to the sharp decline in soil moisture
27 and higher VPD, gross primary productivity (GPP) drops below its normal conditions
28 in the first 16 days and reduces to its minimum within 24 days for more than 50% of
29 the 151 identified flash drought events, and savannas show highest sensitivity to flash
30 drought. Water use efficiency increases for forests but decreases for cropland and
31 savanna during the recovery stage of flash droughts. These results demonstrate the
32 rapid responses of vegetation productivity and resistance of forest ecosystems to flash
33 drought.

34 **Keywords:** Flash drought; GPP; Soil moisture; Water use efficiency; FLUXNET

35 **1. Introduction**

36 Terrestrial ecosystems play a key role in the global carbon cycle and absorb
37 about 30% of anthropogenic carbon dioxide emissions during the past five decades
38 (Le Quéré et al., 2018). With more climate extremes (e.g. droughts, heat waves) in a
39 warming climate, the rate of future land carbon uptake is highly uncertain regardless
40 of the fertilization effect of rising atmospheric carbon dioxide (Green et al., 2019;
41 Reichstein et al., 2013; Xu et al., 2019). Terrestrial ecosystems can even turn to
42 carbon source during extreme drought events (Ciais et al., 2005). Record-breaking
43 drought events have caused enormous reduction of the ecosystem gross primary
44 productivity (GPP), such as the European 2003 drought (Ciais et al., 2005; Reichstein
45 et al., 2007), USA 2012 drought (Wolf et al., 2016), China 2013 drought (Xie et al.,
46 2016; Yuan et al., 2016), Southern Africa 2015/16 drought (Yuan et al., 2017) and
47 Australia Millennium drought (Banerjee et al., 2013). The 2012 summertime drought
48 in USA was classified as flash drought with rapid intensification and insufficient early
49 warning, which caused 26% reduction in crop yield (Hoerling et al., 2014; Otkin et al.,
50 2016). Flash drought may only need several weeks to develop into its maximum
51 intensity, and the rapid onset distinguishes it from traditional drought which is
52 assumed to be a slowly evolving climate phenomenon taking several months or even
53 years to develop (Otkin et al., 2018). Several extreme flash droughts would ultimately
54 propagate into long-term droughts due to persistent precipitation deficits, e.g., 2012
55 flash drought over the USA Midwest Plain (Basara et al., 2019). Flash drought has
56 aroused wide concerns for its unusually rapid development and detrimental effects

57 (Basara et al., 2019; Christian et al., 2019; Ford & Labosier, 2017; Nguyen et al.,
58 2019; Otkin et al., 2018a; Otkin et al., 2018b; Wang and Yuan, 2018; Yuan et al., 2015;
59 Yuan et al., 2017; Yuan et al., 2019b). Despite the increasing occurrence and clear
60 ecological impacts of flash droughts, our understanding of their impacts on carbon
61 uptake in terrestrial ecosystems remains incomplete.

62 Previous studies mainly focused on the response of vegetation to long-term
63 droughts, and found that the response time ranged from several months to years
64 through correlation analysis (Vicente-Serrano et al., 2013; Xu et al., 2018). The
65 response time of vegetation to flash droughts might be different, which requires
66 further investigation for quantification. Recent studies assessed the impact of flash
67 drought on vegetation including the 2012 central USA flash drought and the 2016 and
68 2017 northern USA flash drought. For instance, Otkin et al. (2016) used the
69 evaporative stress index (ESI) to detect the onset of the 2012 central USA flash
70 drought, and found the decline in ESI preceded the drought according to the United
71 States Drought Monitor (Svoboda et al., 2002). He et al. (2019) assessed the impacts
72 of the 2017 northern USA flash drought (which also impacted parts of southern
73 Canada) on vegetation productivity based on GOME-2 solar-induced fluorescence
74 (SIF) and satellite-based evapotranspiration in the US Northern plains. Otkin et al.
75 (2019) examined the evolution of vegetation conditions using LAI from MODIS
76 during the 2015 flash drought over the South-Central United States and found that the
77 LAI decreased after the decline of soil moisture. Besides, the 2016 flash drought over
78 U.S. northern plains also decreased agricultural production (Otkin et al., 2018b).

79 However, previous impact studies only focused on a few extreme flash drought cases
80 without explicit definition of flash drought events. As the baseline climate is changing
81 (Yuan et al., 2019b), it is necessary to systematically investigate the response of
82 terrestrial carbon and water fluxes to flash drought events based on long-term records
83 rather than one or two extreme cases.

84 In fact, there are numerous studies on the influence of drought on ecosystem
85 productivity (Ciais et al., 2005; Stocker et al., 2018; Stocker et al., 2019). It is found
86 that understanding the coupling of water-carbon fluxes during drought is the key to
87 revealing the adaptation and response mechanisms of vegetation to water stress
88 (Boese et al., 2019; Nelson et al., 2018). Water use efficiency (WUE) is the metric for
89 understanding the trade-off between carbon assimilation and water loss through
90 transpiration (Beer et al., 2009; Cowan and Farquhar, 1977; Zhou et al., 2014, 2015),
91 and it is influenced by environmental factors including atmospheric dryness and soil
92 moisture limitations (Boese et al., 2019). Although WUE has been widely studied for
93 seasonal to decadal droughts, few studies have investigated WUE during flash
94 droughts that usually occur at sub-seasonal time scale (Xie et al., 2016; Zhang et al.,
95 2019).

96 In this paper, we address the ecological impact of soil moisture flash droughts
97 through analyzing FLUXNET decade-long observations of CO₂ and water fluxes.
98 Here we consider not only the rapid onset stage of soil moisture flash droughts but
99 also the recovery stage to assess the ecological impacts. The ecological responses to
100 water stress vary under different ecosystems and drought characteristics, and the focus

101 on the soil moisture flash droughts would detect the breakdown of ecosystem
102 functioning of photosynthesis. The specific goals are to (1) examine the response of
103 carbon and water fluxes to soil moisture flash droughts from the onset to the recovery
104 stages, and (2) investigate how WUE changes during soil moisture flash drought for
105 different ecosystems. The methodology proposed by Yuan et al. (2019b) enables the
106 analysis of the flash drought with characteristics of duration, frequency, and intensity
107 in the historical observations. All the flash drought events occurred at the FLUXNET
108 stations are selected to investigate the response of carbon fluxes and WUE. More than
109 10-year records of soil moisture, carbon and water fluxes are available (Baldocchi et
110 al., 2002), which makes it possible to assess the response of vegetation to flash
111 droughts by considering different climates and ecosystem conditions.

112 **2. Data and Methods**

113 **2.1 Data**

114 FLUXNET2015 provides daily hydrometeorological variables including precipitation,
115 temperature, saturation vapor pressure deficit (VPD), soil moisture (sm), shortwave
116 radiation (SW), evapotranspiration (ET) inferred from latent heat, and carbon fluxes
117 including GPP and net ecosystem productivity (NEP). We use GPP data based on
118 night-time partitioning method (GPP_NT_VUT_REF). Considering most sites only
119 measure the surface soil moisture, here we use daily soil moisture measurements
120 mainly at the depth of 5-10 cm averaged from half-hourly data. Soil moisture
121 observations are usually averaged over multiple sensors including time domain
122 reflectometer (TDR), frequency domain reflectometer (FDR), and water content

123 reflectometer etc. However, the older devices may be replaced with newer devices at
124 certain sites, which may decrease the stability of long-term soil moisture observations
125 and the average observation error of soil moisture is $\pm 2\%$. All daily
126 hydrometeorological variables and carbon fluxes are summed to 8-day time scale to
127 study the flash drought impact. There are 34 sites from FLUXNET 2015 dataset
128 (Table 1) consisting of 8 vegetation types, where the periods of observations are no
129 less than 10 years ranging from 1996 to 2014, and the rates of missing data are lower
130 than 5%. Here we only select the FLUXNET observations including 12 evergreen
131 needleleaf forest sites (ENF), 5 deciduous broadleaf forests (DBF), 6 crop sites
132 (CROP; 5 rain-fed sites and 1 irrigated site), 3 mixed forests (MF), and 3 savannas
133 (SAV). The sites for grasslands, evergreen broadleaf forests, and shrublands are
134 excluded because there are less than 10 soil moisture flash drought events. The
135 vegetation classification is according to International Geosphere-Biosphere Program
136 (IGBP; Belward et al., 1999), where MF is dominated by neither deciduous nor
137 evergreen tree type with tree cover larger than 60% and the land tree cover is 10-30%
138 for SAV. The detailed information is listed in Table 1.

139 **2.2 Methods**

140 **2.2.1 Definition of soil moisture flash drought events**

141 The definition of soil moisture flash drought should account for both its rapid
142 intensification and the drought conditions (Otkin et al., 2018a; Yuan et al., 2019b).
143 Here we used soil moisture percentile to identify soil moisture flash drought
144 according to Yuan et al. (2019b) and Ford et al. (2017). Figure 1 shows the procedure

145 for soil moisture flash drought identification, including five criteria to identify the
146 rapid onset and recovery stages of soil moisture flash drought. 1) Soil moisture flash
147 drought starts at the middle day of the 8-day period when the 8-day mean soil
148 moisture is less than the 40th percentile, and the 8-day mean soil moisture prior to the
149 starting time should be higher than 40th percentile to ensure the transition from a
150 non-drought condition. 2) The mean decreasing rate of 8-day mean soil moisture
151 percentile should be no less than 5% per 8 days to address the rapid drought
152 intensification. 3) The 8-day mean soil moisture after the rapid decline should be less
153 than 20% in percentile, and the period from the beginning to the end of the rapid
154 decline is regarded as the onset stage of soil moisture flash drought (those within red
155 dashed line in Figure 1). 4) If the mean decreasing rate is less than 5% in percentile or
156 the soil moisture percentile starts to increase, the soil moisture flash drought enters
157 into the “recovery” stage, and the soil moisture flash drought event (as well as the
158 recovery stage) ends when soil moisture recovers to above 20th percentile (those
159 within blue dashed line in Figure 1). The recovery stage is also crucial to assess the
160 impact of soil moisture flash drought (Yuan et al., 2019b). 5) The minimum duration
161 of a flash drought event is 24 days to exclude those dry spells that last for a too short
162 period to cause any impacts.

163 At least decade-long observations of 8-day mean soil moisture are used to
164 calculate soil moisture percentile with a moving window of 8-day before and 8-day
165 after the target 8-day, resulting in at least 30 samples for deriving the cumulative
166 distribution function of soil moisture before calculating percentiles. Besides, the target

167 8-day soil moisture percentiles are only based on the target 8-day soil moisture in the
168 context of the expanded samples. For example, the soil moisture percentile of June
169 22nd in 1998 is calculated by firstly ranking June 14th, June 22nd, and June 30th soil
170 moisture in all historical years (N samples) from lowest to highest, identifying the
171 rank of soil moisture of June 22nd, 1998 (e.g., M), and obtaining the percentile as
172 $M/N*100$. We focus on growing seasons during April-September for sites in the North
173 Hemisphere and October-March for sites in the South Hemisphere.

174 **2.2.2 Response time of GPP to soil moisture flash drought**

175 Drought has a large influence on ecosystem productivity through altering the plant
176 photosynthesis and ecosystem respiration (Beer et al., 2010; Green et al., 2019;
177 Heimann & Reichstein, 2008; Stocker et al., 2018). GPP dominates the global
178 terrestrial carbon sink and it would decrease due to stomatal closure and non-stomatal
179 limitations like reduced carboxylation rate and reduced active leaf area index (de la
180 Motte et al., 2019) under water stress. The negative anomalies of GPP during soil
181 moisture flash drought are considered as the onset of ecological response. Here, we
182 use two response time indices to investigate the relationship between soil moisture
183 flash drought and ecological drought (Crausbay et al., 2017; Niu et al., 2018; Song et
184 al., 2018; Vicente-Serrano et al., 2013): 1) the response time of the first occurrence
185 (RT) of negative standardized GPP anomaly ($SGPPA = \frac{GPP - \mu_{GPP}}{\sigma_{GPP}}$, where μ_{GPP} and
186 σ_{GPP} are mean and standard deviation of the time series of GPP at the same dates as
187 the target 8-days for all years, which can remove the influence of seasonality. For
188 instance, all Apr 1-8 during 1996-2014 would have a μ_{GPP} and a σ_{GPP} based on a

189 climatology same as soil moisture percentile calculation which consists of March
190 24-31, Apr 1-8, and Apr 9-16 in all years, and Apr 9-16 would have another μ_{GPP}
191 and another σ_{GPP} , and so on), which is the lag time between the start of flash drought
192 and the time when SGPPA becomes negative during flash drought period; and 2) the
193 response time of occurrence of minimum SGPPA (RTmin), which is the lag time
194 between the start of flash drought and the time when SGPPA decreases to its
195 minimum values during the flash drought period. If the response time is 8 days for the
196 first occurrence of negative SGPPA, it means that the response of GPP starts at the
197 beginning of flash drought (the first time step of flash drought). Considering flash
198 drought is identified through surface soil moisture due to the availability of
199 FLUXNET data, vegetation with deeper roots may obtain water in deep soil and
200 remain healthy during flash drought. The roots vary among different vegetation types
201 and forests are assumed to have deeper roots than grasslands, which may influence the
202 response to soil moisture flash droughts.

203 **2.2.3 Water use efficiency**

204 Carbon assimilation and transpiration are coupled by stomates, and plants face a
205 tradeoff between carbon uptake through photosynthesis and water loss through
206 transpiration under the influence of water and energy availability (Boese et al., 2019;
207 Gentine et al., 2019; Huang et al., 2016; Nelson et al., 2018). WUE can be used to
208 quantify the trade-off between carbon and water cycles, and is defined as the
209 assimilated amount of carbon per unit of water loss (Peters et al., 2018). At the
210 ecosystem scale, WUE is the ratio of GPP over ET (Cowan and Farquhar, 1977).

211 Drought would cause stomatal closure and non-stomatal adjustments in biochemical
 212 functions thus altering the coupling between GPP and ET. Underlying WUE (uWUE)
 213 is calculated as $GPP \times \sqrt{VPD}/ET$ considering the nonlinear relationship between
 214 GPP, VPD and ET (Zhou et al., 2014). uWUE is supposed to reflect the relationship of
 215 photosynthesis-transpiration via stomatal conductance at the ecosystem level by
 216 considering the effect of VPD on WUE (Beer et al., 2009; Boese et al., 2019; Zhou et
 217 al., 2014, 2015). WUE varies under the influence of VPD on canopy conductance
 218 (Beer et al., 2009; Tang et al., 2006), whereas uWUE is considered to remove this
 219 effect and be more directly linked with the relationship between environmental
 220 conditions (e.g., soil moisture) and plant conditions (e.g., carboxylation rate; Lu et al.,
 221 2018). The standardized anomalies of WUE and uWUE are calculated the same as
 222 SGPPA, where different sites have different mean values and standard deviations for
 223 different target 8-days to remove the spatial and temporal inhomogeneity.

224 **2.2.4 The relations between meteorological conditions and GPP**

225 Considering the compound impacts of temperature, radiation, VPD and soil
 226 moisture on vegetation photosynthesis, the partial correlation is used to investigate the
 227 relationship between GPP and each climate factor, with the other 3 climate factors as
 228 control variables as follows:

$$229 \quad r_{ij(m_1, m_2, \dots, m_n)} = \frac{r_{ij(m_1, \dots, m_{n-1})} - r_{im_n(m_1, \dots, m_{n-1})} r_{jm_n(m_1, \dots, m_{n-1})}}{\sqrt{(1 - r_{in(m_1, \dots, m_{n-1})}^2)(1 - r_{jn(m_1, \dots, m_{n-1})}^2)}} \quad (1)$$

230 where i represents GPP, j represents the target meteorological variables and
 231 m_1, m_2, \dots, m_n represent the control meteorological variables. $r_{ij(m_1, m_2, \dots, m_n)}$ is the
 232 partial correlation coefficient between i and j , and $r_{ij(m_1, \dots, m_{n-1})}$, $r_{im_n(m_1, \dots, m_{n-1})}$ and

233 $r_{jm_n(m_1, \dots, m_{n-1})}$ are partial correlation coefficients between i and j , i and m_n , j and
234 m_n respectively under control of m_1, m_2, \dots and m_{n-1} .

235 **3. Results**

236 **3.1 Identification of flash drought events at FLUXNET stations**

237 Based on FLUXNET data, we have identified 151 soil moisture flash drought
238 events with durations longer than or equal to 24 days using soil moisture observations
239 of 371 site years. Figure 2a shows the distribution of the 29 sites with different
240 vegetation types, which are mainly distributed over North America and Europe. The
241 number of soil moisture flash drought ranges from 13 to 70 events among different
242 vegetation types. There are 12 ENF sites in this study, and the number of soil moisture
243 flash droughts for ENF (70) is the most among all the vegetation types. The duration
244 for flash drought events ranges from 24 days to several months. In some extreme
245 cases, the flash droughts would develop into long-term droughts without enough
246 rainfall to alleviate drought conditions. Mean durations of soil moisture flash droughts
247 for different vegetation types range from around 30 days to 50 days (Figure 2c).

248 Figure 3 shows the meteorological conditions during different stages of soil
249 moisture flash drought including the standardized anomalies of temperature,
250 precipitation, VPD, and shortwave radiation and soil moisture percentiles. Here the
251 onset and recovery stages of flash droughts refer to certain periods characterized by
252 the soil moisture decline rates. The standardized anomalies of temperature,
253 precipitation, VPD, and shortwave and soil moisture percentiles are composited to
254 show the meteorological conditions during different stages of flash droughts. The

255 onset stage of soil moisture flash droughts mainly refers to the rapid intensification,
256 and the flash droughts may or may not develop into long-term droughts depending on
257 the deficits in precipitation. There is a slight reduction in precipitation during 8 days
258 prior to soil moisture flash drought (Figure 3b). During the onset of soil moisture
259 flash drought, soil moisture percentiles decline rapidly from nearly 50% during 8 days
260 before flash drought to 18% during onset stages (Figure 3e). The rapid drying of soil
261 moisture is always associated with a large precipitation deficits, anomalously high
262 temperature and shortwave radiation and large VPD indicate increased atmospheric
263 dryness (Ford et al., 2017; Koster et al., 2019; Wang et al., 2016), which persist until
264 the recovery stage except for shortwave radiation. The soil moisture percentiles are
265 averaged during the onset and recovery stages and the soil moisture percentiles during
266 recovery stages are slightly lower than those during onset stages (Figure 3e)
267 considering the soil moisture is not quite dry during the early period of onset stages.
268 Sufficient precipitation occurs during the 8 days after soil moisture flash droughts to
269 relieve the drought condition and soil moisture percentiles increase from 12% during
270 recovery stages to 36% during 8 days after flash droughts.

271 **3.2 Climatological statistics of the response time of GPP to flash drought**

272 By analyzing all the 151 soil moisture flash drought events across 29 FLUXNET
273 sites, we find that negative GPP anomalies occur during 81% of the soil moisture
274 flash drought events. Figure 4 shows the probability distributions of the response time
275 of GPP to soil moisture flash drought as determined by soil moisture reductions for
276 the first occurrence of negative SGPPA, the minimum negative value of SGPPA and

277 the minimum soil moisture percentiles for different vegetation types, respectively. To
278 reduce the uncertainty due to small sample sizes, only the results for vegetation types
279 (SAV, CROP, MF, DBF, ENF) with more than 10 flash drought events are shown. For
280 soil moisture flash droughts from all vegetation types, the first occurrences of
281 negative SGPPA are concentrated during the first 24 days, and GPP starts to respond
282 to soil moisture flash drought within 16 days for 57% flash droughts (Figures 4a-e).
283 The occurrences of minimum value of SGPPA rise sharply at the beginning of soil
284 moisture flash drought, and reach the peak during 17-24 days, and then slow down
285 (Figures 4f-j), which is similar to the decline in soil moisture. Although the first
286 occurrences of negative SGPPA mainly occur in the onset stage, GPP would continue
287 to decrease in the recovery stages for 60% of soil moisture flash drought events.
288 Different types of vegetation including herbaceous plants and woody plants all react
289 to soil moisture flash drought in the early stage (Figures 4a-e). Among them, SAV
290 shows the fastest reaction to water stress (Figures 4a and 4f), and the RT is within 8
291 days for 63% events, suggesting that SAV responds concurrently with soil moisture
292 flash drought onset. Ultimately, 88% events for SAV show reduced vegetation
293 photosynthesis. The result is consistent with previous studies regarding the strong
294 response of semi-arid ecosystems to water availability (Gerken et al., 2019;
295 Vicente-Serrano et al., 2013; Zeng et al., 2018), and the decline in GPP for SAV is
296 related to isohydric behaviors during soil moisture drought and higher VPD, through
297 closing stomata to decrease water loss as transpiration and carbon assimilation
298 (Novick et al., 2016; Roman et al., 2015). For ENF, only 27% of soil moisture flash

299 droughts cause the negative SGPPA during the first 8 days. When RT is within 40
300 days, the cumulative frequencies range from 74% to 88% among different vegetation
301 types. The response frequency of RT_{min} and the response time of minimum soil
302 moisture percentiles are quite similar, although there are discrepancies among the
303 patterns of the response frequency for different vegetation types. The response
304 frequency of RT_{min} for SAV increases sharply during 17-24 days of soil moisture
305 flash droughts (Figure 4f). GPP is derived from direct eddy covariance observations
306 of NEP and nighttime terrestrial ecosystem respiration, and temperature-fitted
307 terrestrial ecosystem respiration during daytime. The response of NEP to flash
308 droughts shows the compound effects of vegetation photosynthesis and ecosystem
309 respiration. In terms of RT, the response of NEP is slower than GPP for SAV, but is
310 quicker for DBF and ENF (Figure 5). The discrepancies between NEP and SM in
311 terms of RT_{min} are more obvious than those between GPP and SM, and the RT_{min} of
312 NEP is much shorter than the RT_{min} of soil moisture especially for DBF and ENF,
313 which may be related to the increase of ecosystem respiration (Figures 5 i and j).

314 Figure 6 shows the temporal changes of SGPPA and soil moisture percentiles
315 during 8 days before soil moisture flash droughts and during the first 24 days of the
316 droughts. During 8 days before flash droughts, there is nearly no obvious decline for
317 SGPPA, while SAV, DBF and ENF shows small increase in GPP. The decline in
318 SGPPA is more significant during the first 9-24 days of soil moisture flash droughts
319 for different vegetation types, and SGPPA for SAV and CROP show quicker decline
320 even during the first 8 days of soil moisture flash droughts. The decline rates in soil

321 moisture are mainly concentrated within the first 16 days of flash droughts. There are
322 various lag times for the response of GPP to the decline in soil moisture among
323 different vegetation.

324 **3.3 The coupling between carbon and water fluxes under soil moisture stress**

325 Figure 7 shows the standardized anomalies of WUE and uWUE and their
326 components for different ecosystems during 8 days before and after soil moisture
327 flash droughts and the onset and recovery stages. Here, we select 81% of soil moisture
328 flash drought events with GPP declining down to its normal conditions to analyze the
329 interactions between carbon and water fluxes, while GPP during the remaining 19%
330 of soil moisture flash drought events may stay stable and is less influenced by drought
331 conditions. During 8 days before soil moisture flash drought, WUE and uWUE are
332 generally close to the climatology (Figure 7a) and there are no significant changes in
333 GPP, ET, and ET/\sqrt{VPD} (Figures 7e and 7i). However, the median value of SGPPA
334 for SAV is positive (Figure 7e). WUE is stable during the onset stage, whereas uWUE
335 increases for all ecosystems except for CROP (Figure 7b). For CROP, both GPP and
336 ET decrease, and the decline in WUE is related with a greater reduction in GPP
337 relative to ET (Figure 7f and 7j). The positive anomalies of uWUE are correlated with
338 decrease in ET/\sqrt{VPD} mainly induced by the high VPD. Increasing VPD and
339 deficits in soil moisture would decrease canopy conductance (Grossiord et al., 2020)
340 but not GPP for MF and ENF. During the onset stage, GPP and ET reduce only for
341 SAV, and CROP, and DBF, and the magnitudes of GPP and ET reduction are highest
342 for SAV. ET is close to normal conditions for MF, DBF, and ENF, thus enhancing the

343 drying rate of soil moisture with less precipitation supply during the onset stage. But
344 during recovery stage of soil moisture flash drought, GPP and ET show significant
345 reductions except for MF (Figures 7g and 7k), and the responses of WUE and uWUE
346 are different between herbaceous plants (SAV and CROP) and forests (MF, DBF, and
347 ENF), where WUE and uWUE decrease significantly for SAV and CROP but increase
348 slightly for forests (Figure 7c). The decrease in uWUE for SAV and CROP during
349 recovery stages indicates that SAV and CROP are likely brown due to carbon
350 starvation caused by the significant decrease in stomatal conductance (McDowell et
351 al., 2008). The decrease in GPP during recovery stage is not only related to the
352 reduction in canopy conductance, but also the decrease in uWUE under drought for
353 SAV and CROP which is possibly influenced by suppressed state of enzyme and
354 reduced mesophyll conductance (Flexas et al., 2012). However, the positive
355 anomalies of uWUE for DBF and ENF during the recover stage imply that the decline
356 in GPP mainly results from the stomata closure. ET starts to decrease during the
357 recovery stage due to the limitation of water availability, and the decreasing ET also
358 reflects the enhanced water stress for vegetation during the recovery stage. The
359 average soil moisture conditions are 12% in percentile for recovery stage but 18% for
360 onset stage. So, drier soil moisture in the recovery stage exacerbates ecological
361 response. Figure 7c also shows the higher WUE and uWUE for forests, which
362 indicates their higher resistance to flash drought than herbaceous plants during
363 recovery stage. During 8 days after flash drought, the standardized anomalies of
364 uWUE are still positive for forests, whereas SGPPA and ET are both lower than the

365 climatology for all ecosystems. The ecological negative effect would persist after the
366 soil moisture flash drought.

367 **3.4 The impact of climate factors on GPP during soil moisture flash drought**

368 Figure 8 shows the partial correlation coefficients between standardized
369 anomalies of GPP and meteorological variables and soil moisture percentiles during
370 different stages of soil moisture flash droughts. The correlation between climate
371 factors and GPP is not statistically significant during 8 days before soil moisture flash
372 droughts. During onset stages of soil moisture flash droughts, the partial correlation
373 coefficients between SGPPA and soil moisture percentiles are 0.44, 0.49 and 0.29,
374 respectively for SAV, CROP, and ENF ($p < 0.05$). Besides, shortwave radiation is
375 positively correlated with SGPPA for MF, DBF, and EBF (Figure 8b) during onset
376 stages and the positive anomalies of shortwave radiation could partially offset the loss
377 of vegetation photosynthesis due to the deficits in soil moisture. SGPP is also
378 positively correlated with temperature during onset stages for SAV and DBF. The
379 partial correlation coefficients between SGPPA and VPD are -0.53 and -0.22
380 respectively for DBF and ENF, and the higher VPD would further decrease GPP
381 during onset stages. The influence of VPD on GPP is much more significant during
382 recovery stages and 8 days after. SGPPA is positively correlated with soil moisture
383 and negatively with VPD for SAV both during recovery stages and 8 days after.

384 **4. Discussion**

385 Previous studies detected the vegetation response for a few extreme drought cases
386 without a specific definition of flash drought from a climatological perspective (Otkin

387 et al., 2016; He et al., 2019). Moreover, less attention has been paid to the coupling
388 between carbon and water fluxes during soil moisture flash drought events. This study
389 investigates the response of carbon and water fluxes to soil moisture flash drought
390 based on decade-long FLUXNET observations during different stages of flash
391 droughts. The responses vary across different phases of flash drought, and different
392 ecosystems have different responses, which provide implications for eco-hydrological
393 modeling and prediction. Besides, the influence of different climate factors including
394 VPD and soil moisture also differs during different stages of soil moisture flash
395 droughts.

396 **4.1 The responses of carbon and water fluxes to flash droughts**

397 Based on 151 soil moisture flash drought events identified using soil moisture
398 from decade-long FLUXNET observations, the response of GPP to flash drought is
399 found to be quite rapid. For more than half of the 151 soil moisture flash drought
400 events, the GPP drops below its normal conditions during the first 16 days and
401 reaches its maximum reduction within 24 days. Due to the influence of ecosystem
402 respiration, the responses of NEP for DBF and ENF to flash droughts are much
403 quicker than GPP, implying that the sensitivity of ecosystem respiration is less than
404 that of vegetation photosynthesis (Granier et al., 2007). Eventually, 81% of soil
405 moisture flash drought events cause declines in GPP. During the drought period,
406 plants would close their stomata to minimize water loss through decreasing canopy
407 conductance, which in turn leads to a reduction in carbon uptake. The soil moisture
408 flash droughts are always accompanied by high temperature and VPD. The partial

409 correlation analysis shows that the increase in VPD and decrease in soil moisture both
410 decrease the rate of photosynthesis. High VPD further reduces canopy conductance to
411 minimize water loss at the cost of reducing photosynthesis during soil moisture flash
412 drought (Grossiord et al., 2020). The suppression of GPP and ET is more obvious for
413 flash drought recovery stage determined by soil moisture than the onset stage. The
414 discrepancy of GPP responses between different phases of soil moisture flash drought
415 may result from 1) soil moisture conditions which are drier during the recovery stage,
416 and 2) the damaged physiological functioning for specific vegetation types. The
417 anomalies of uWUE for ecosystems are always positive or unchanged during soil
418 moisture flash drought except for croplands and savannas during recovery stage. The
419 decrease in canopy conductance would limit photosynthetic rate, however, the
420 increase of uWUE may indicate adaptative regulations of ecosystem physiology
421 which is consistent with Beer et al. (2009). uWUE is higher than WUE during onset
422 stage of soil moisture flash drought, which is due to the decreased conductance under
423 increased VPD. However, there is no obvious difference between WUE and uWUE
424 during recovery stage, which indicates that photosynthesis is less sensitive to stomatal
425 conductance and may be more correlated with limitations of biochemical capacity
426 (Flexas et al., 2012; Grossiord et al., 2020). During 8 days after the soil moisture flash
427 drought, the anomalies of GPP and ET are still negative, indicating that the vegetation
428 does not recover immediately after the soil moisture flash drought. The legacy effects
429 of flash droughts may be related to the vegetation and climate conditions (Barnes et
430 al., 2016; Kannenberg et al., 2020).

431 This study is based on the sites that are mainly distributed over North America
432 and Europe. It is necessary to investigate the impact of flash drought on vegetation
433 over other regions with different climates and vegetation conditions. In addition, this
434 study used in-situ surface soil moisture at FLUXNET stations to detect vegetation
435 response due to the lack of soil moisture observations at deep soil layers. There would
436 be more significant ecological responses to flash drought identified through using
437 root-zone soil moisture because of its close link with vegetation dynamics. Due to the
438 limitation of FLUXNET soil moisture measurements, here we used soil moisture
439 observations mainly at the depths of 5 to 10 cm. We also analyzed the response of
440 GPP to flash drought identified by 0.25-degree ERA5 soil moisture reanalysis data at
441 the depths of 7cm and 1m. The response of GPP to flash droughts identified by
442 FLUXNET surface soil moisture are quite similar to those identified by ERA5 soil
443 moisture at the depth of 1m (not shown). There are less GPP responses to flash
444 droughts identified by ERA5 surface soil moisture. Although we select the ERA5 grid
445 cell that is closest to the FLUXNET site and use the ERA5 soil moisture data over the
446 same period as the FLUXNET data, we should acknowledge that the gridded ERA5
447 data might not be able to represent the soil moisture conditions as well as flash
448 droughts at in-situ scale due to strong heterogeneity of land surface. Therefore, the
449 in-situ surface soil moisture from FLUXNET is useful to identify flash droughts
450 compared with reanalysis soil moisture, although the in-situ root-zone soil moisture
451 would be better.

452 **4.2 Variation in ecological responses across vegetation types**

453 The responses of GPP, ET and WUE to soil moisture flash drought vary among
454 different vegetation types. The decline in GPP and ET only occurs across croplands
455 and savannas during onset stage. For most forests, the deterioration of photosynthesis
456 and ET appears during the recovery stage with higher WUE and uWUE. For CROP
457 and SAV, both WUE and uWUE decrease during the recovery stage and they may be
458 brown due to reduced photosynthesis. The positive anomalies of WUE and uWUE for
459 forests suggest that their deeper roots can obtain more water than grasslands during
460 flash drought. Xie et al. (2016) pointed out that WUE and uWUE for a subtropical
461 forest increased during the 2013 summer drought in southern China. The increased
462 WUE in forest sites and unchanged WUE in grasslands were also found in other
463 studies for spring drought (Wolf et al., 2013). In general, herbaceous plants are more
464 sensitive to flash drought than forests, especially for savannas. The correlation
465 between soil moisture and GPP is more significant for SAV, CROP, and ENF during
466 onset stages of flash droughts, which is consistent with the strong response to water
467 availability of SAV and CROP (Gerken et al., 2019). SAV is more isohydric than
468 forests and would reduce stomatal conductance immediately to prohibit water loss
469 that further exacerbates drought (Novick et al., 2016; Roman et al., 2015). However,
470 almost all vegetation types show high sensitivity to VPD during the recovery stage of
471 flash droughts.

472 **4.3 Potential implications for ecosystem modelling**

473 The study reveals the profound impact of soil moisture flash droughts on
474 ecosystem through analyzing eddy covariance observations. It is found that the

475 responses of carbon and water exchanges are quite distinguishing for forests and
476 herbaceous plants. For the ecosystem modeling, the response of stomatal conductance
477 under soil moisture stress has been addressed in previous studies (Wilson et al., 2000),
478 but there still exists deficiency to capture the impacts of water stress on carbon uptake
479 (Keenan et al., 2009), which is partly due to the different responses across species.
480 Incorporating physiological adaptations to drought in ecosystem modeling especially
481 for forests would improve the simulation of the impact of drought on the terrestrial
482 ecosystems.

483 **5. Conclusion**

484 This study presents how carbon and water fluxes respond to soil moisture flash
485 drought during 8 days before flash droughts, onset and recovery stages, and 8 days
486 after flash droughts through analyzing decade-long observations from FLUXNET.
487 Ecosystems show high sensitivity of GPP to soil moisture flash drought especially for
488 savannas, and GPP starts to respond to soil moisture flash droughts within 16 days for
489 more than half of the flash drought events under the influence of the deficit in soil
490 moisture and higher VPD. However, the responses of WUE and uWUE vary across
491 vegetation types. Positive WUE and uWUE anomalies for forests during the recovery
492 stage indicate the resistance to soil moisture flash drought through non-stomatal
493 regulations, whereas WUE and uWUE decrease for croplands and savannas during the
494 recovery stage. For now, the main concern about the ecological impact of soil
495 moisture flash drought is concentrated on the period of flash drought and the legacy
496 effects of flash drought are not involved. It still needs more efforts to study the

497 subsequent effects of soil moisture flash droughts which would contribute to assessing
498 the accumulated ecological impacts of flash drought. Nevertheless, this study
499 highlights the rapid response of vegetation productivity to soil moisture dynamics at
500 sub-seasonal timescale, and different responses of water use efficiency across
501 ecosystems during the recovery stage of soil moisture flash droughts, which
502 complements previous studies on the sensitivity of vegetation to extreme drought at
503 longer time scale. Understanding the response of carbon fluxes and the coupling
504 between carbon and water fluxes to drought, especially considering the effects of
505 climate change and human interventions (Yuan et al., 2020), might help assessing the
506 resistance and resilience of vegetation to drought.

507

508 **Acknowledgements**

509 The authors thank two anonymous reviewers for their helpful comments, and thank Dr.
510 Zhenzhong Zeng for his constructive suggestions. This work was supported by
511 National Natural Science Foundation of China (41875105), National Key R&D
512 Program of China (2018YFA0606002) and the Startup Foundation for Introducing
513 Talent of NUIST. The data used in this study are all from FLUXNET 2015
514 (<https://fluxnet.fluxdata.org/data/fluxnet2015-dataset/>).

515

516 **Data availability statement**

517 Carbon fluxes and hydrometeorological variables from FLUXNET2015 are available
518 through <https://fluxnet.fluxdata.org/data/fluxnet2015-dataset/>.

519 **References**

- 520 Atjay, G. L., Ketner, P. and Duvigneaud, P.: Terrestrial primary production and
521 phytomass, in *The Global Carbon Cycle: SCOPE 13*, John Wiley, Hoboken, N. J.,
522 129–182, 1979
- 523 Baldocchi, D., Wilson, K., Valentini, R., Law, B., Munger, W., Davis, K., Wofsy, S.,
524 Pilegaard, K., Goldstein, A., Falge, E., Vesala, T., Hollinger, D., Running, S.,
525 Fuentes, J., Katul, G., Gu, L., Verma, S., Paw, K. T., Malhi, Y., Anthoni, P.,
526 Oechel, W., Schmid, H. P., Bernhofer, C., Meyers, T., Evans, R., Olson, R. and
527 Lee, X.: FLUXNET: A New Tool to Study the Temporal and Spatial Variability
528 of Ecosystem–Scale Carbon Dioxide, Water Vapor, and Energy Flux Densities,
529 *Bull. Am. Meteorol. Soc.*, 82(11), 2415–2434, <https://doi.org/10.1175/1520-0477>,
530 2002.
- 531 Banerjee, O., Bark, R., Connor, J. and Crossman, N. D.: An ecosystem services
532 approach to estimating economic losses associated with drought, *Ecol. Econ.*, 91,
533 19–27, <https://doi.org/10.1016/j.ecolecon.2013.03.022>, 2013.
- 534 Barnes, M. L., Moran, M. S., Scott, R. L., Kolb, T. E., Ponce-Campos, G. E., Moore,
535 D. J. P., Ross, M. A., Mitra, B. and Dore, S.: Vegetation productivity responds to
536 sub-annual climate conditions across semiarid biomes, *Ecosphere*, 7(5), 1–20,
537 <https://doi.org/10.1002/ecs2.1339>, 2016
- 538 Basara, J. B., Christian, J. I., Wakefield, R. A., Otkin, J. A., Hunt, E. H. H. and Brown,
539 D. P.: The evolution, propagation, and spread of flash drought in the Central
540 United States during 2012, *Environ. Res. Lett.*, 14(8),

541 <https://doi.org/10.1088/1748-9326/ab2cc0>, 2019.

542 Belward, A. S., Estes, J. E., and Kline, K. D.: The igbp-dis global 1-km land-cover
543 data set discover: A project overview. *Photogramm Eng Rem S*, 65(9):1013–
544 1020, 1999

545 Beer, C., Ciais, P., Reichstein, M., Baldocchi, D., Law, B. E., Papale, D., Soussana, J.
546 F., Ammann, C., Buchmann, N., Frank, D., Gianelle, D., Janssens, I. A., Knohl,
547 A., Köstner, B., Moors, E., Rouspard, O., Verbeeck, H., Vesala, T., Williams, C.
548 A. and Wohlfahrt, G.: Temporal and among-site variability of inherent water use
549 efficiency at the ecosystem level, *Global Biogeochem. Cycles*, 23(2), 1–13,
550 <https://doi.org/10.1029/2008GB003233>, 2009.

551 Beer, C., Reichstein, M., Tomelleri, E., Ciais, P., Jung, M., Carvalhais, N., Rödenbeck,
552 C., Arain, M. A., Baldocchi, D., Bonan, G. B., Bondeau, A., Cescatti, A., Lasslop,
553 G., Lindroth, A., Lomas, M., Luysaert, S., Margolis, H., Oleson, K. W.,
554 Rouspard, O., Veenendaal, E., Viovy, N., Williams, C., Woodward, F. I. and
555 Papale, D.: Terrestrial gross carbon dioxide uptake: Global distribution and
556 covariation with climate, *Science*, 329(5993), 834–838,
557 <https://doi.org/10.1126/science.1184984>, 2010.

558 Boese, S., Jung, M., Carvalhais, N., Teuling, A. J. and Reichstein, M.: Carbon-water
559 flux coupling under progressive drought, *Biogeosciences*, 16(13), 2557–2572,
560 <https://doi.org/10.5194/bg-16-2557-2019>, 2019.

561 Cowan, I. R. and Farquhar, G. D.: Stomatal function in relation to leaf metabolism
562 and environment, in *Integration of Activity in the Higher Plant*, edited by D. H.

563 Jennings, Cambridge Univ. Press, Cambridge, U. K., 471–505, 1977

564 Christian, J. I., Basara, J. B., Otkin, J. A., Hunt, E. D., Wakefield, R. A., Flanagan, P.
565 X. and Xiao, X.: A methodology for flash drought identification: Application of
566 flash drought frequency across the United States, *J. Hydrometeorol.*, 20(5), 833–
567 846, <https://doi.org/10.1175/JHM-D-18-0198.1>, 2019.

568 Ciais, P., Reichstein, M., Viovy, N., Granier, A., Ogée, J., Allard, V., Aubinet, M.,
569 Buchmann, N., Bernhofer, C., Carrara, A., Chevallier, F., De Noblet, N., Friend,
570 A. D., Friedlingstein, P., Grünwald, T., Heinesch, B., Keronen, P., Knohl, A.,
571 Krinner, G., Loustau, D., Manca, G., Matteucci, G., Miglietta, F., Ourcival, J. M.,
572 Papale, D., Pilegaard, K., Rambal, S., Seufert, G., Soussana, J. F., Sanz, M. J.,
573 Schulze, E. D., Vesala, T. and Valentini, R.: Europe-wide reduction in primary
574 productivity caused by the heat and drought in 2003, *Nature*, 437(7058), 529–
575 533, <https://doi.org/10.1038/nature03972>, 2005.

576 Crausbay, S. D., Ramirez, A. R., Carter, S. L., Cross, M. S., Hall, K. R., Bathke, D. J.,
577 Betancourt, J. L., Colt, S., Cravens, A. E., Dalton, M. S., Dunham, J. B., Hay, L.
578 E., Hayes, M. J., McEvoy, J., McNutt, C. A., Moritz, M. A., Nislow, K. H.,
579 Raheem, N. and Sanford, T.: Defining ecological drought for the twenty-first
580 century, *Bull. Am. Meteorol. Soc.*, 98(12), 2543–2550,
581 <https://doi.org/10.1175/BAMS-D-16-0292.1>, 2017.

582 de la Motte, L. G., Beauclaire, Q., Heinesch, B., Cuntz, M., Foltýnová, L., Šigut, L.,
583 Kowalska, N., Manca, G., Ballarin, I. G., Vincke, C., Roland, M., Ibrom, A.,
584 Lousteau, D., Siebicke, L. and Longdoz, B.: Non-stomatal processes reduce

585 gross primary productivity in temperate forest ecosystems during severe edaphic
586 drought, *Philos. Trans. R. Soc. B*, <https://doi.org/10.1098/RSTB-2019-0527>,
587 2019.

588 Flexas, J., Barbour, M. M., Brendel, O., Cabrera, H. M., Carriqui í M., D áz-Espejo, A.,
589 Douthe, C., Dreyer, E., Ferrio, J. P., Gago, J., Gall é A., Galm és, J., Kodama, N.,
590 Medrano, H., Niinemets, Ü., Peguero-Pina, J. J., Pou, A., Ribas-Carbó, M.,
591 Tomás, M., Tosens, T. and Warren, C. R.: Mesophyll diffusion conductance to
592 CO₂: An unappreciated central player in photosynthesis, *Plant Sci.*, 193–194,
593 70–84, <https://doi.org/10.1016/j.plantsci.2012.05.009>, 2012.

594 Ford, T. W. and Labosier, C. F.: Meteorological conditions associated with the onset
595 of flash drought in the Eastern United States, *Agric. For. Meteorol.*, 247(April),
596 414–423, <https://doi.org/10.1016/j.agrformet.2017.08.031>, 2017.

597 Ford, T. W., McRoberts, D. B., Quiring, S. M. and Hall, R. E.: On the utility of in situ
598 soil moisture observations for flash drought early warning in Oklahoma, USA,
599 *Geophys. Res. Lett.*, 42(22), <https://doi.org/10.1002/2015GL066600>, 2015.

600 Granier, A., Reichstein, M., Br áda, N., Janssens, I. A., Falge, E., Ciais, P., Grünwald,
601 T., Aubinet, M., Berbigier, P., Bernhofer, C., Buchmann, N., Facini, O., Grassi,
602 G., Heinesch, B., Ilvesniemi, H., Keronen, P., Knohl, A., Köstner, B., Lagergren,
603 F., Lindroth, A., Longdoz, B., Loustau, D., Mateus, J., Montagnani, L., Nys, C.,
604 Moors, E., Papale, D., Peiffer, M., Pilegaard, K., Pita, G., Pumpanen, J., Rambal,
605 S., Rebmann, C., Rodrigues, A., Seufert, G., Tenhunen, J., Vesala, T. and Wang,
606 Q.: Evidence for soil water control on carbon and water dynamics in European

607 forests during the extremely dry year: 2003, *Agric. For. Meteorol.*, 143(1–2),
608 123–145, <https://10.1016/j.agrformet.2006.12.004>, 2007.

609 Gentine, P., Green, J. K., Gu érin, M., Humphrey, V., Seneviratne, S. I., Zhang, Y. and
610 Zhou, S.: Coupling between the terrestrial carbon and water cycles - A review,
611 *Environ. Res. Lett.*, 14(8), <https://10.1088/1748-9326/ab22d6>, 2019.

612 Gerken, T., Ruddell, B. L., Yu, R., Stoy, P. C. and Drewry, D. T.: Robust observations
613 of land-to-atmosphere feedbacks using the information flows of FLUXNET,
614 *Clim. Atmos. Sci.*, 2(37), <https://doi.org/10.1038/s41612-019-0094-4>, 2019.

615 Green, J. K., Seneviratne, S. I., Berg, A. M., Findell, K. L., Hagemann, S., Lawrence,
616 D. M. and Gentine, P.: Large influence of soil moisture on long-term terrestrial
617 carbon uptake, *Nature*, 565(7740), 476–479,
618 <https://doi.org/10.1038/s41586-018-0848-x>, 2019.

619 Grossiord, C., Buckley, T. N., Cernusak, L. A., Novick, K. A., Poulter, B., Siegwolf, R.
620 T. W., Sperry, J. S. and McDowell, N. G.: Plant responses to rising vapor
621 pressure deficit, *New Phytol.*, <https://doi.org/10.1111/nph.16485>, 2020.

622 He, M., Kimball, J. S., Yi, Y., Running, S., Guan, K., Jenco, K., Maxwell, B. and
623 Maneta, M.: Impacts of the 2017 flash drought in the US Northern plains
624 informed by satellite-based evapotranspiration and solar-induced fluorescence,
625 *Environ. Res. Lett.*, 14(7), 074019, <https://doi.org/10.1088/1748-9326/ab22c3>,
626 2019.

627 Heimann, M. and Reichstein, M.: Terrestrial ecosystem carbon dynamics and climate
628 feedbacks, *Nature*, 451(7176), 289–292, <https://doi.org/10.1038/nature06591>,

629 2008.

630 Hoerling, M., Eischeid, J., Kumar, A., Leung, R., Mariotti, A., Mo, K., Schubert, S.
631 and Seager, R.: Causes and predictability of the 2012 great plains drought, *Bull.*
632 *Am. Meteorol. Soc.*, 95(2), 269–282,
633 <https://doi.org/10.1175/BAMS-D-13-00055.1>, 2014.

634 Huang, M., Piao, S., Zeng, Z., Peng, S., Ciais, P., Cheng, L., Mao, J., Poulter, B., Shi,
635 X., Yao, Y., Yang, H. and Wang, Y.: Seasonal responses of terrestrial ecosystem
636 water-use efficiency to climate change, *Glob. Chang. Biol.*, 22(6), 2165–2177,
637 <https://doi.org/10.1111/gcb.13180>, 2016.

638 Keenan, T., Garc ía, R., Friend, A. D., Zaehle, S., Gracia, C. and Sabate, S.: Improved
639 understanding of drought controls on seasonal variation in mediterranean forest
640 canopy CO₂ and water fluxes through combined in situ measurements and
641 ecosystem modelling, *Biogeosciences*, 6(8), 1423–1444,
642 <https://doi.org/10.5194/bg-6-1423-2009>, 2009.

643 Koster, R. D., Schubert, S. D., Wang, H., Mahanama, S. P. and DeAngelis, A. M.:
644 Flash Drought as Captured by Reanalysis Data: Disentangling the Contributions
645 of Precipitation Deficit and Excess Evapotranspiration, *J. Hydrometeorol.*, 20(6),
646 1241–1258, <https://doi.org/10.1175/jhm-d-18-0242.1>, 2019.

647 Kannenberg, S. A., Schwalm, C. R. and Anderegg, W. R. L.: Ghosts of the past: how
648 drought legacy effects shape forest functioning and carbon cycling, *Ecol. Lett.*,
649 *ele.13485*, <https://doi.org/10.1111/ele.13485>, 2020.

650 McDowell, N., Pockman, W. T., Allen, C. D., Breshears, D. D., Cobb, N., Kolb, T.,

651 Plaut, J., Sperry, J., West, A., Williams, D. G. and Yezzer, E. A.: Mechanisms of
652 plant survival and mortality during drought: Why do some plants survive while
653 others succumb to drought?, *New Phytol.*, 178(4), 719–739,
654 <https://doi.org/10.1111/j.1469-8137.2008.02436.x>, 2008.

655 Novick, K. A., Ficklin, D. L., Stoy, P. C., Williams, C. A., Bohrer, G., Oishi, A. C.,
656 Papuga, S. A., Blanken, P. D., Noormets, A., Sulman, B. N., Scott, R. L., Wang,
657 L. and Phillips, R. P.: The increasing importance of atmospheric demand for
658 ecosystem water and carbon fluxes, *Biogeosciences*, 13(September), 1–5,
659 <https://doi.org/10.1038/NCLIMATE3114>, 2016.

660 Nelson, J. A., Carvalhais, N., Migliavacca, M., Reichstein, M. and Jung, M.:
661 Water-stress-induced breakdown of carbon-water relations: Indicators from
662 diurnal FLUXNET patterns, *Biogeosciences*, 15(8), 2433–2447,
663 <https://doi.org/10.5194/bg-15-2433-2018>, 2018.

664 Nguyen, H., Wheeler, M. C., Otkin, J. A., Cowan, T., Frost, A. and Stone, R.: Using
665 the evaporative stress index to monitor flash drought in Australia, *Environ. Res.
666 Lett.*, 14(6), <https://doi.org/10.1088/1748-9326/ab2103>, 2019.

667 Niu, J., Chen, J., Sun, L. and Sivakumar, B.: Time-lag effects of vegetation responses
668 to soil moisture evolution: a case study in the Xijiang basin in South China,
669 *Stoch. Environ. Res. Risk Assess.*, 32(8), 2423–2432,
670 <https://doi.org/10.1007/s00477-017-1492-y>, 2018.

671 Otkin, J. A., Anderson, M. C., Hain, C., Mladenova, I. E., Basara, J. B. and Svoboda,
672 M.: Examining Rapid Onset Drought Development Using the Thermal Infrared–

673 Based Evaporative Stress Index, *J. Hydrometeorol.*, 14(4), 1057–1074,
674 <https://doi.org/10.1175/JHM-D-12-0144.1>, 2013.

675 Otkin, J. A., Anderson, M. C., Hain, C., Svoboda, M., Johnson, D., Mueller, R.,
676 Tadesse, T., Wardlow, B. and Brown, J.: Assessing the evolution of soil moisture
677 and vegetation conditions during the 2012 United States flash drought, *Agric. For.*
678 *Meteorol.*, 218–219, 230–242, <https://doi.org/10.1016/j.agrformet.2015.12.065>,
679 2016.

680 Otkin, J. A., Svoboda, M., Hunt, E. D., Ford, T. W., Anderson, M. C., Hain, C. and
681 Basara, J. B.: Flash droughts: A review and assessment of the challenges
682 imposed by rapid-onset droughts in the United States, *Bull. Am. Meteorol. Soc.*,
683 99(5), 911–919, <https://doi.org/10.1175/BAMS-D-17-0149.1>, 2018a.

684 Otkin, J. A., Haigh, T., Mucia, A., Anderson, M. C. and Hain, C.: Comparison of
685 Agricultural Stakeholder Survey Results and Drought Monitoring Datasets
686 during the 2016 U.S. Northern Plains Flash Drought, *Weather. Clim. Soc.*, 10(4),
687 867–883, <https://doi.org/10.1175/wcas-d-18-0051.1>, 2018b.

688 Otkin, J. A., Zhong, Y., Hunt, E. D., Basara, J., Svoboda, M., Anderson, M. C. and
689 Hain, C.: Assessing the Evolution of Soil Moisture and Vegetation Conditions
690 during a Flash Drought–Flash Recovery Sequence over the South-Central United
691 States, *J. Hydrometeorol.*, 20(3), 549–562,
692 <https://doi.org/10.1175/jhm-d-18-0171.1>, 2019.

693 Qu ´ e ´ C., Andrew, R., Friedlingstein, P., Sitch, S., Hauck, J., Pongratz, J., Pickers, P.,
694 Ivar Korsbakken, J., Peters, G., Canadell, J., Arneth, A., Arora, V., Barbero, L.,

695 Bastos, A., Bopp, L., Ciais, P., Chini, L., Ciais, P., Doney, S., Gkritzalis, T., Goll,
696 D., Harris, I., Haverd, V., Hoffman, F., Hoppema, M., Houghton, R., Hurtt, G.,
697 Ilyina, T., Jain, A., Johannessen, T., Jones, C., Kato, E., Keeling, R., Klein
698 Goldewijk, K., Landschützer, P., Lefèvre, N., Lienert, S., Liu, Z., Lombardozzi,
699 D., Metzl, N., Munro, D., Nabel, J., Nakaoka, S. I., Neill, C., Olsen, A., Ono, T.,
700 Patra, P., Pregon, A., Peters, W., Peylin, P., Pfeil, B., Pierrot, D., Poulter, B.,
701 Rehder, G., Resplandy, L., Robertson, E., Rocher, M., Rödenbeck, C., Schuster,
702 U., Skjelvan, I., Sférian, R., Skjelvan, I., Steinhoff, T., Sutton, A., Tans, P., Tian,
703 H., Tilbrook, B., Tubiello, F., Van Der Laan-Luijkx, I., Van Der Werf, G., Viovy,
704 N., Walker, A., Wiltshire, A., Wright, R., Zaehle, S. and Zheng, B.: Global
705 Carbon Budget 2018, *Earth Syst. Sci. Data*, 10(4), 2141–2194,
706 <https://doi.org/10.5194/essd-10-2141-2018>, 2018.

707 Peters, W., van der Velde, I. R., van Schaik, E., Miller, J. B., Ciais, P., Duarte, H. F.,
708 van der Laan-Luijkx, I. T., van der Molen, M. K., Scholze, M., Schaefer, K.,
709 Vidale, P. L., Verhoef, A., Wårlind, D., Zhu, D., Tans, P. P., Vaughn, B. and
710 White, J. W. C.: Increased water-use efficiency and reduced CO₂ uptake by
711 plants during droughts at a continental scale, *Nat. Geosci.*, 11(10), 744–748,
712 <https://10.1038/s41561-018-0212-7>, 2018.

713 Reichstein, M., Ciais, P., Papale, D., Valentini, R., Running, S., Viovy, N., Cramer, W.,
714 Granier, A., Ogée, J., Allard, V., Aubinet, M., Bernhofer, C., Buchmann, N.,
715 Carrara, A., Grünwald, T., Heimann, M., Heinesch, B., Knohl, A., Kutsch, W.,
716 Loustau, D., Manca, G., Matteucci, G., Miglietta, F., Ourcival, J. M., Pilegaard,

717 K., Pumpanen, J., Rambal, S., Schaphoff, S., Seufert, G., Soussana, J. F., Sanz,
718 M. J., Vesala, T. and Zhao, M.: Reduction of ecosystem productivity and
719 respiration during the European summer 2003 climate anomaly: A joint flux
720 tower, remote sensing and modelling analysis, *Glob. Chang. Biol.*, 13(3), 634–
721 651, <https://doi.org/10.1111/j.1365-2486.2006.01224.x>, 2007.

722 Reichstein, M., Bahn, M., Ciais, P., Frank, D., Mahecha, M. D., Seneviratne, S. I.,
723 Zscheischler, J., Beer, C., Buchmann, N., Frank, D. C., Papale, D., Rammig, A.,
724 Smith, P., Thonicke, K., Van Der Velde, M., Vicca, S., Walz, A. and Wattenbach,
725 M.: Climate extremes and the carbon cycle, *Nature*, 500(7462), 287–295,
726 <https://doi.org/10.1038/nature12350>, 2013.

727 Roman, D. T., Novick, K. A., Brzostek, E. R., Dragoni, D., Rahman, F. and Phillips, R.
728 P.: The role of isohydric and anisohydric species in determining ecosystem-scale
729 response to severe drought, *Oecologia*, 179(3), 641–654,
730 <https://doi.org/10.1007/s00442-015-3380-9>, 2015.

731 Saleska, S. R., Didan, K., Huete, A. R. and Da Rocha, H. R.: Amazon forests green-up
732 during 2005 drought, *Science*, 318(5850), 612, doi:10.1126/science.1146663,
733 2007.

734 Sippel, S., Reichstein, M., Ma, X., Mahecha, M. D., Lange, H., Flach, M. and Frank,
735 D.: Drought, Heat, and the Carbon Cycle: a Review, *Curr. Clim. Chang. Reports*,
736 4(3), 266–286, <https://doi.org/10.1007/s40641-018-0103-4>, 2018.

737 Song, L., Luis, G., Guan, K., You, L., Huete, A., Ju, W. and Zhang, Y.: Satellite
738 sun-induced chlorophyll fluorescence detects early response of winter wheat to

739 heat stress in the Indian Indo-Gangetic Plains, *Glob. Chang. Biol.*, 24, 4023–
740 4037, <https://doi.org/10.1111/gcb.14302>, 2018.

741 Stocker, B. D., Zscheischler, J., Keenan, T. F., Prentice, I. C., Peñuelas, J. and
742 Seneviratne, S. I.: Quantifying soil moisture impacts on light use efficiency
743 across biomes, *New Phytol.*, 218(4), 1430–1449,
744 <https://doi.org/10.1111/nph.15123>, 2018.

745 Stocker, B. D., Zscheischler, J., Keenan, T. F., Prentice, I. C., Seneviratne, S. I. and
746 Peñuelas, J.: Drought impacts on terrestrial primary production underestimated
747 by satellite monitoring, *Nat. Geosci.*, 12, 274-270,
748 <https://doi.org/10.1038/s41561-019-0318-6>, 2019.

749 Vicente-Serrano, S. M., Gouveia, C., Camarero, J. J., Beguería, S., Trigo, R.,
750 López-Moreno, J. I., Azorín-Molina, C., Pasho, E., Lorenzo-Lacruz, J., Revuelto,
751 J., Morán-Tejeda, E. and Sanchez-Lorenzo, A.: Response of vegetation to
752 drought time-scales across global land biomes, *Proc. Natl. Acad. Sci. U. S. A.*,
753 110(1), 52–57, <https://doi.org/10.1073/pnas.1207068110>, 2013.

754 Wang, L. and Yuan, X.: Two Types of Flash Drought and Their Connections with
755 Seasonal Drought, *Adv. Atmos. Sci.*, 35(12), 1478–1490,
756 <https://doi.org/10.1007/s00376-018-8047-0>, 2018.

757 Wang, L., Yuan, X., Xie, Z., Wu, P. and Li, Y.: Increasing flash droughts over China
758 during the recent global warming hiatus, *Sci. Rep.*, 6, 30571,
759 <https://doi.org/10.1038/srep30571>, 2016.

760 Wilson, K. B., Baldocchi, D. D. and Hanson, P. J.: Quantifying stomatal and

761 non-stomatal limitations to carbon assimilation resulting from leaf aging and
762 drought in mature deciduous tree species, *Tree Physiol.*, 20, 787–797,
763 <https://doi.org/10.1093/treephys/20.12.787>, 2000.

764 Wolf, S., Eugster, W., Ammann, C., Häni, M., Zielis, S., Hiller, R., Stieger, J., Imer, D.,
765 Merbold, L. and Buchmann, N.: Erratum: Contrasting response of grassland
766 versus forest carbon and water fluxes to spring drought in Switzerland
767 (*Environmental Research Letters* (2013) 8 (035007)), *Environ. Res. Lett.*, 9(8),
768 <https://doi.org/10.1088/1748-9326/9/8/089501>, 2014.

769 Wolf, S., Keenan, T. F., Fisher, J. B., Baldocchi, D. D., Desai, A. R., Richardson, A.
770 D., Scott, R. L., Law, B. E., Litvak, M. E. and Brunsell, N. A.: Warm spring
771 reduced carbon cycle impact of the 2012 US summer drought, 113(21),
772 5880-5885, <https://doi.org/10.1073/pnas.1519620113>, 2016.

773 Xie, Z., Wang, L., Jia, B. and Yuan, X.: Measuring and modeling the impact of a
774 severe drought on terrestrial ecosystem CO₂ and water fluxes in a subtropical
775 forest, *J. Geophys. Res. Biogeosciences*, 121(10), 2576–2587,
776 <https://doi.org/10.1002/2016JG003437>, 2016.

777 Xu, C., McDowell, N. G., Fisher, R. A., Wei, L., Sevanto, S., Christoffersen, B. O.,
778 Weng, E. and Middleton, R. S.: Increasing impacts of extreme droughts on
779 vegetation productivity under climate change, *Nat. Clim. Chang.*,
780 <https://doi.org/10.1038/s41558-019-0630-6>, 2019.

781 Xu, H. jie, Wang, X. ping, Zhao, C. yan and Yang, X. mei: Diverse responses of
782 vegetation growth to meteorological drought across climate zones and land

783 biomes in northern China from 1981 to 2014, *Agric. For. Meteorol.*, 262, 1–13,
784 <https://10.1016/j.agrformet.2018.06.027>, 2018.

785 Yuan, W., Cai, W., Chen, Y., Liu, S., Dong, W., Zhang, H., Yu, G., Chen, Z., He, H.,
786 Guo, W., Liu, D., Liu, S., Xiang, W., Xie, Z., Zhao, Z. and Zhou, G.: Severe
787 summer heatwave and drought strongly reduced carbon uptake in Southern
788 China, *Sci. Rep.*, 6, 18813, <https://doi.org/10.1038/srep18813>, 2016.

789 Yuan, W., Zheng, Y., Piao, S., Ciais, P., Lombardozzi, D., Wang, Y., Ryu, Y., Chen, G.,
790 Dong, W., Hu, Z., Jain, A. K., Jiang, C., Kato, E., Li, S., Lienert, S., Liu, S.,
791 Nabel, J. E. M. S., Qin, Z., Quine, T., Sitch, S., Smith, W. K., Wang, F., Wu, C.,
792 Xiao, Z. and Yang, S.: Increased atmospheric vapor pressure deficit reduces
793 global vegetation growth, *Sci. Adv.*, 5(8), eaax1396,
794 <https://doi.org/10.1126/sciadv.aax1396>, 2019a.

795 Yuan, X., Ma, Z., Pan, M. and Shi, C.: Microwave remote sensing of flash droughts
796 during crop growing seasons, 17, 8196, <https://doi.org/10.1002/2015GL064125>,
797 2015.

798 Yuan, X., Wang, L. and Wood, E. F.: Anthropogenic intensification of southern
799 African flash droughts as exemplified by the 2015/16 season, *Bull. Am. Meteorol.*
800 *Soc.*, <https://doi.org/10.1175/BAMS-D-17-007.1>, 2017.

801 Yuan, X., Wang, L., Wu, P., Ji, P., Sheffield, J. and Zhang, M.: Anthropogenic shift
802 towards higher risk of flash drought over China, *Nat. Commun.*, 10(1),
803 <https://doi.org/10.1038/s41467-019-12692-7>, 2019b.

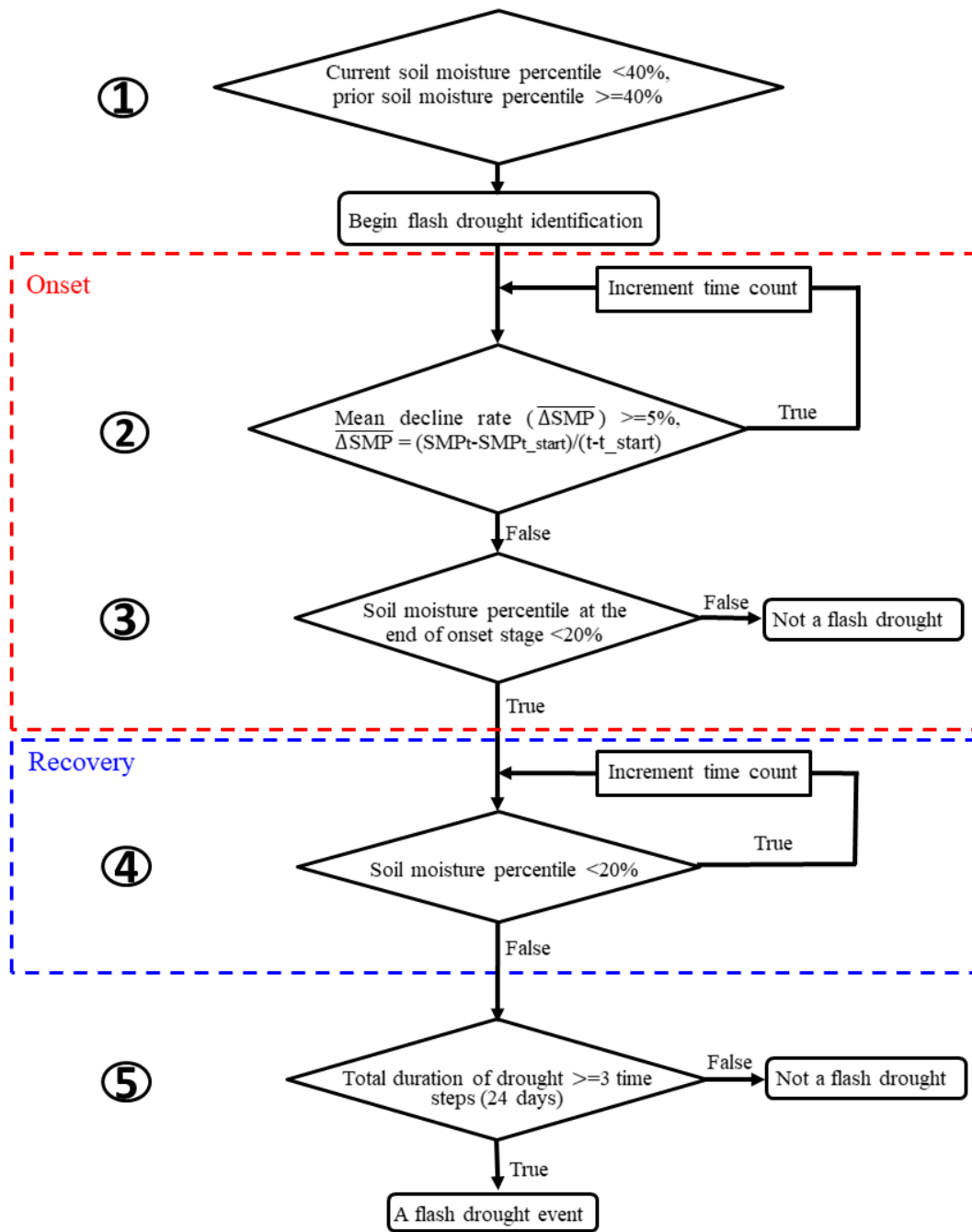
804 Yuan, X., Ma, F., Li, H., et al.: A review on multi-scale drought processes and predicti

805 on under global change. *Trans. Atmos. Sci.*, 43(1), 225-237, <https://doi.org/10.13>
806 [878/j.cnki.dqkxxb.20191105005](https://doi.org/10.13878/j.cnki.dqkxxb.20191105005) (in Chinese), 2020

807 Zeng, Z., Piao, S., Li, L. Z. X., Wang, T., Ciais, P., Lian, X., Yang, Y., Mao, J., Shi, X.
808 and Myneni, R. B.: Impact of Earth greening on the terrestrial water cycle, *J.*
809 *Clim.*, 31(7), 2633–2650, <https://doi.org/10.1175/JCLI-D-17-0236.1>, 2018.

810 Zhou, S., Yu, B., Huang, Y. and Wang, G.: The effect of vapor pressure deficit on
811 water use efficiency at the subdaily time scale, *Geophys. Res. Lett.*, 41(14),
812 5005–5013, <https://doi.org/10.1002/2014GL060741>, 2014.

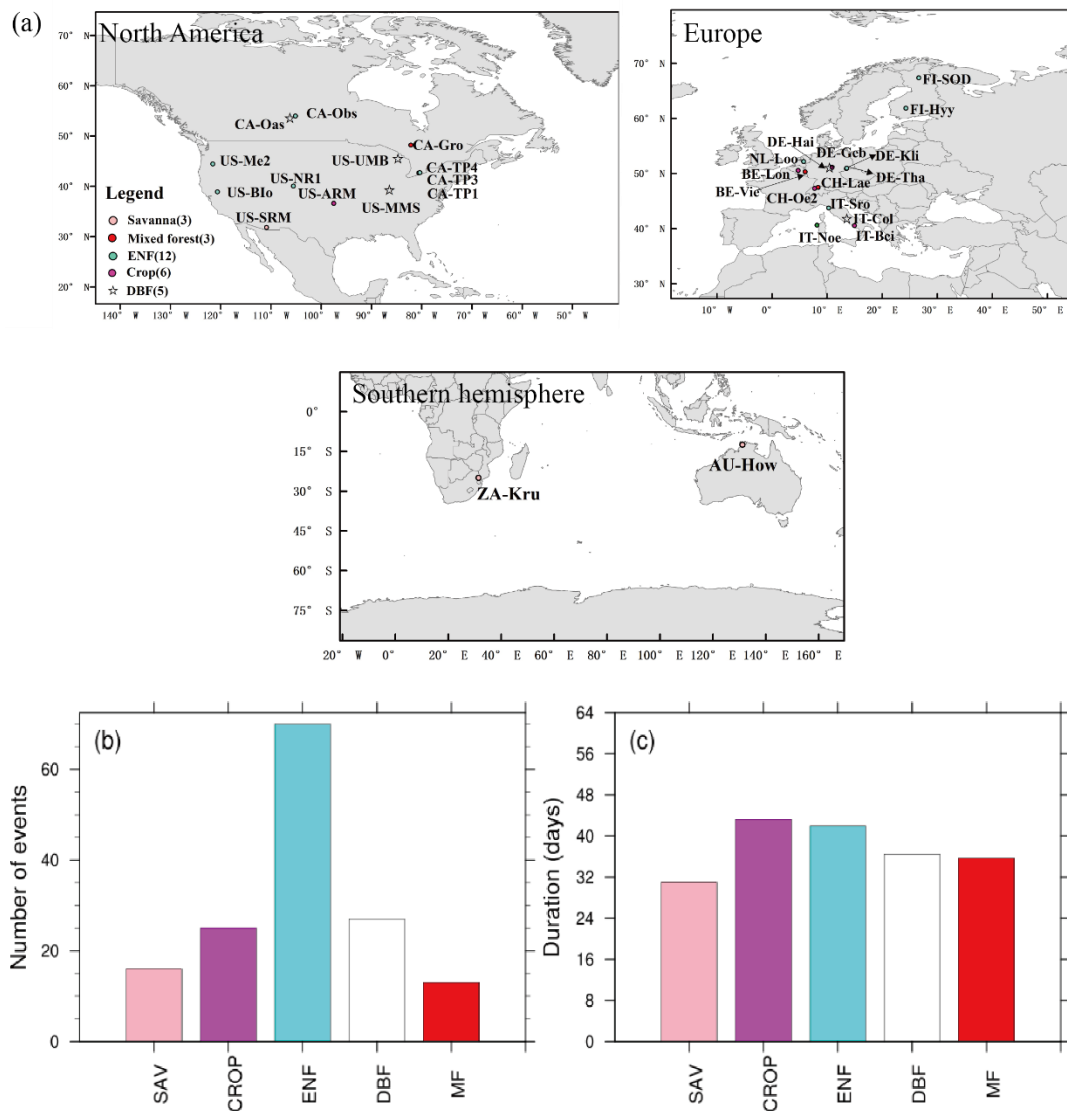
813 Zhou, S., Bofu, Y., Huang, Y. and Wang, G.: Daily underlying water use efficiency for
814 AmeriFlux sites, *J. Geophys. Res. Biogeosciences*, 120, 887–902,
815 <https://doi.org/10.1002/2015JG002947>, 2015.



816

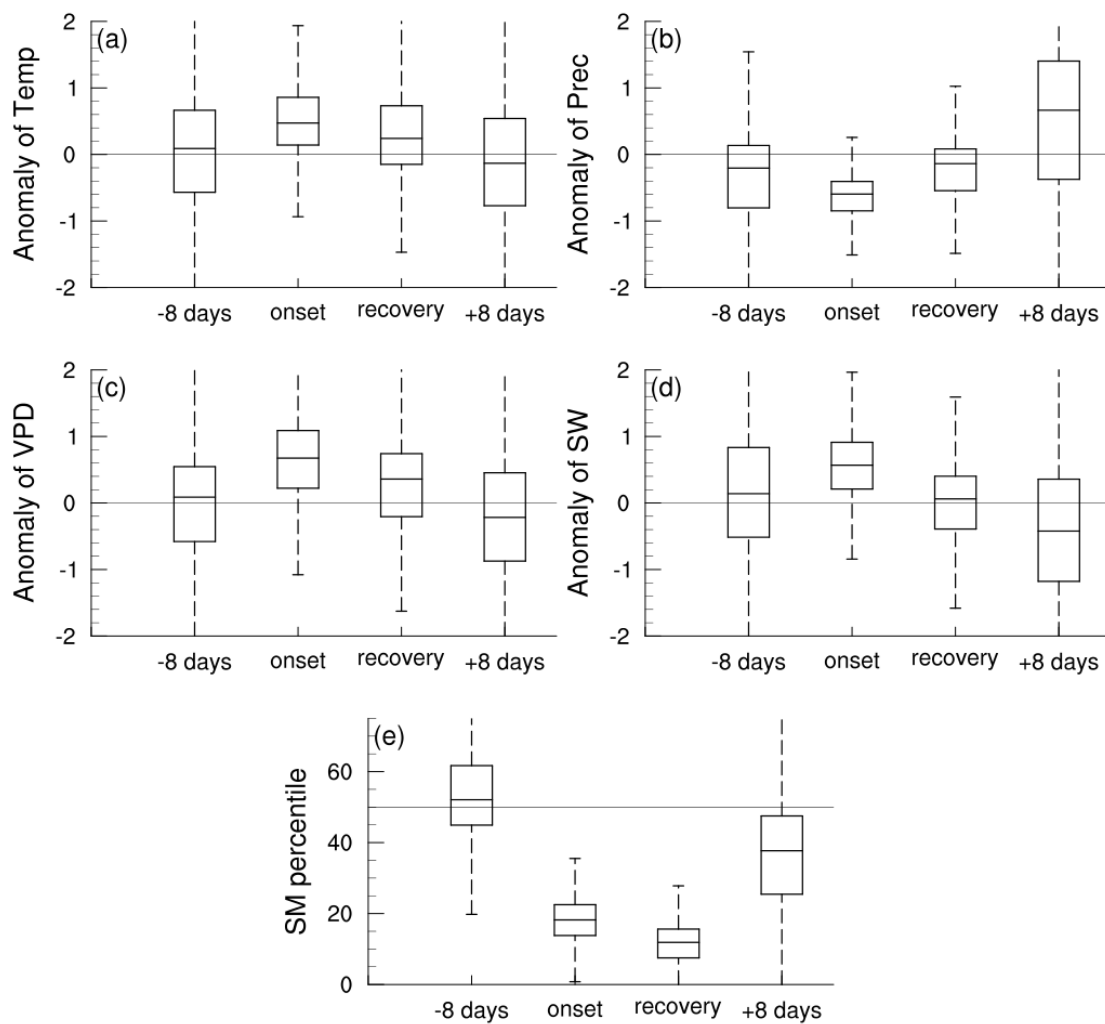
817 **Figure 1.** A flowchart of flash drought identification by considering soil moisture

818 decline rate and drought persistency.



819

820 **Figure 2.** Global map of 29 FLUXNET sites used in this study (a) and flash drought
 821 characteristics (b&c). (b) Total numbers (events) and (c) mean durations (days) of
 822 flash drought events for each vegetation type during their corresponding periods (see
 823 Table 1 for details). Different colors represent different vegetation types.



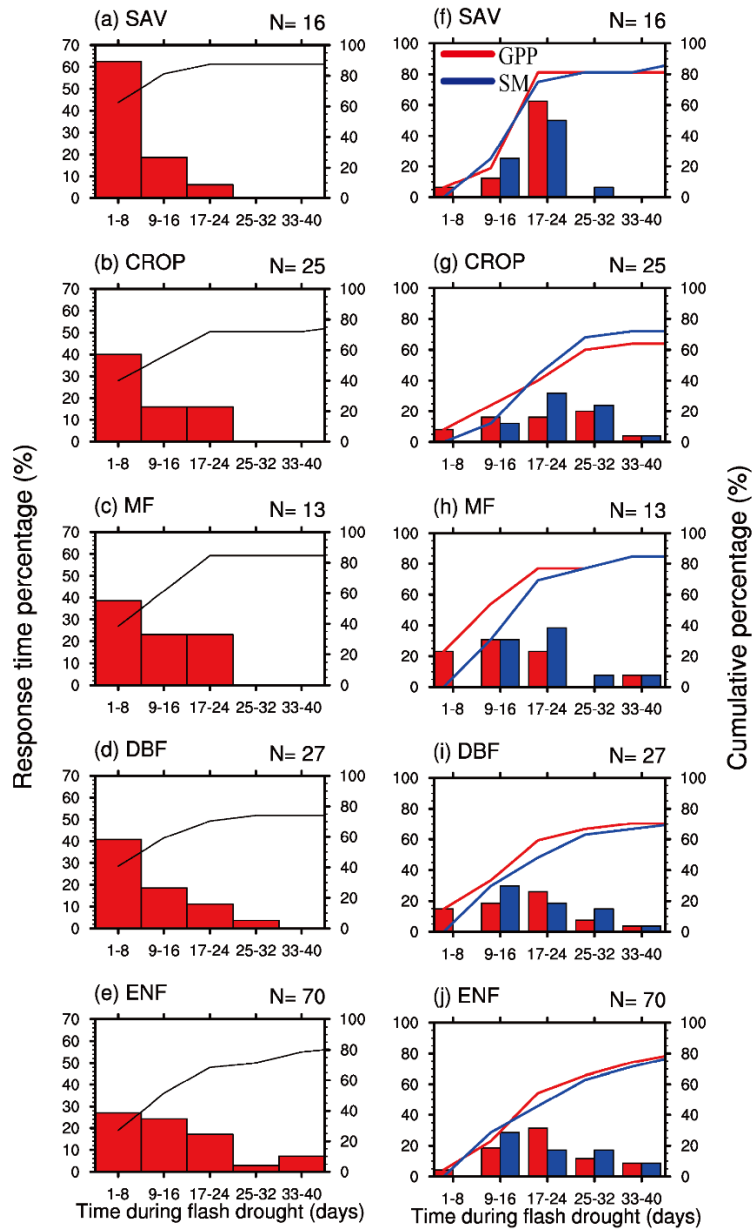
824

825 **Figure 3.** Standardized 8-day anomalies of (a) temperature, (b) precipitation, (c) VPD,

826 (d) short wave radiation (SW), and (e) soil moisture (SM) percentiles during 8 days

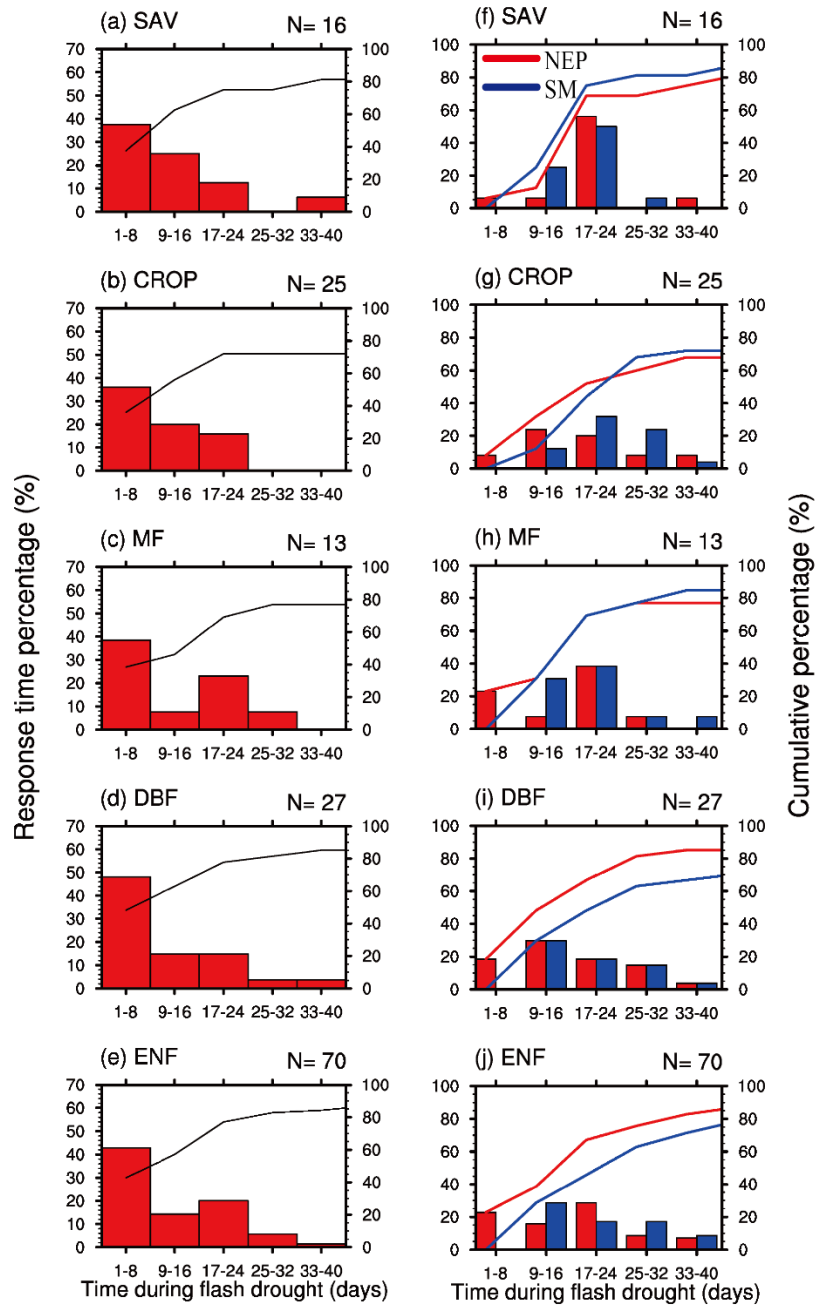
827 prior to flash drought onset, onset and recovery stages of flash drought, and 8 days

828 after flash drought.



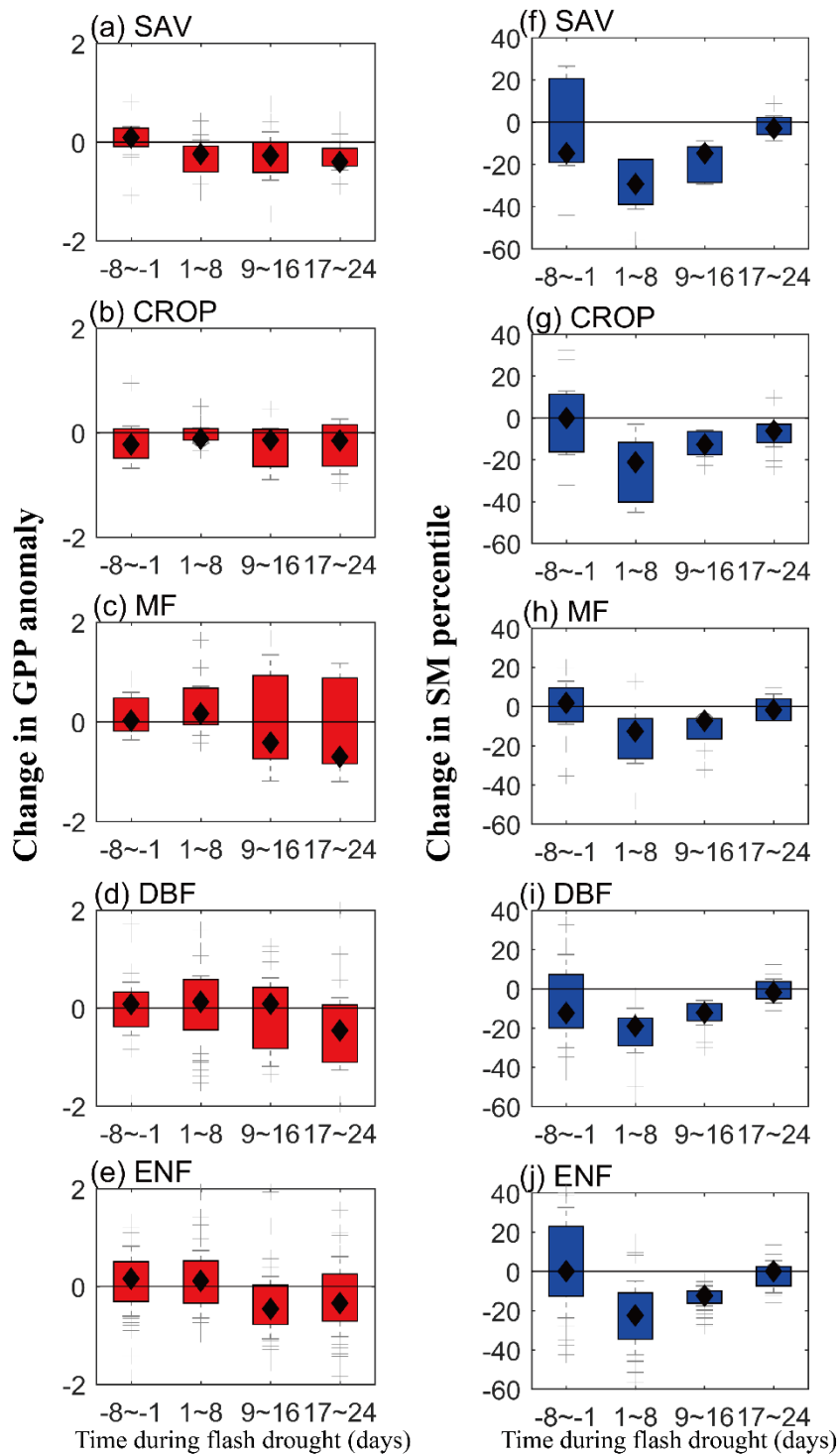
829

830 **Figure 4.** Percentage of the response time (days) of the first occurrence of negative
 831 GPP anomaly (a-e), minimum GPP anomaly and minimum soil moisture percentile
 832 (f-j) during soil moisture flash drought for different vegetation types. SAV: savanna,
 833 CROP: rainfed cropland, MF: mixed forest, DBF: deciduous broadleaf forest and
 834 ENF: evergreen needleleaf forest.



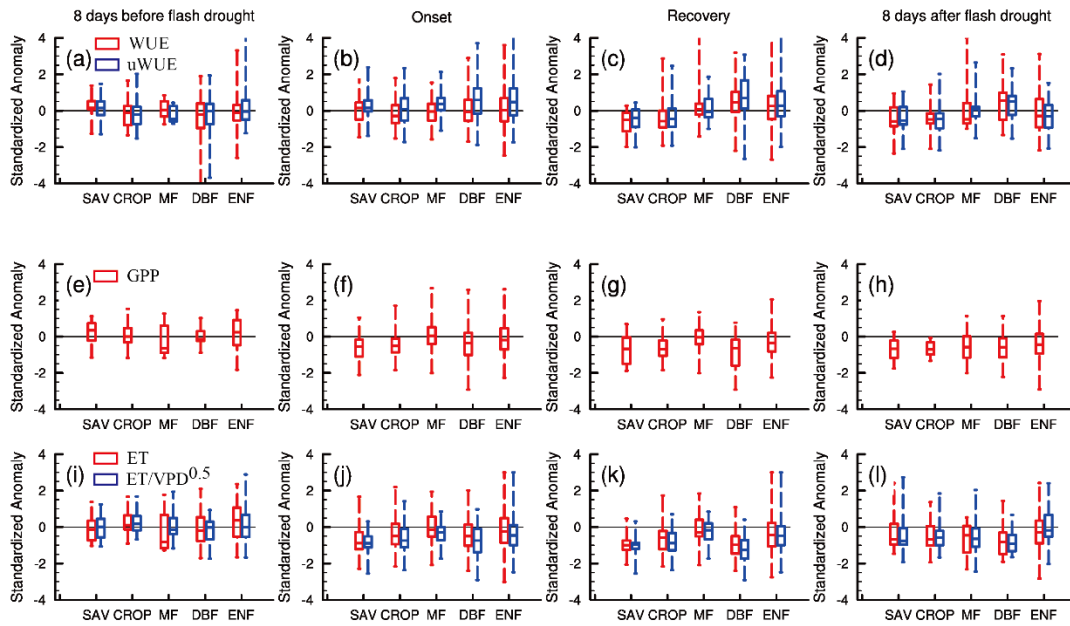
835

836 **Figure 5.** The same as Figure 4, but for net ecosystem productivity (NEP).



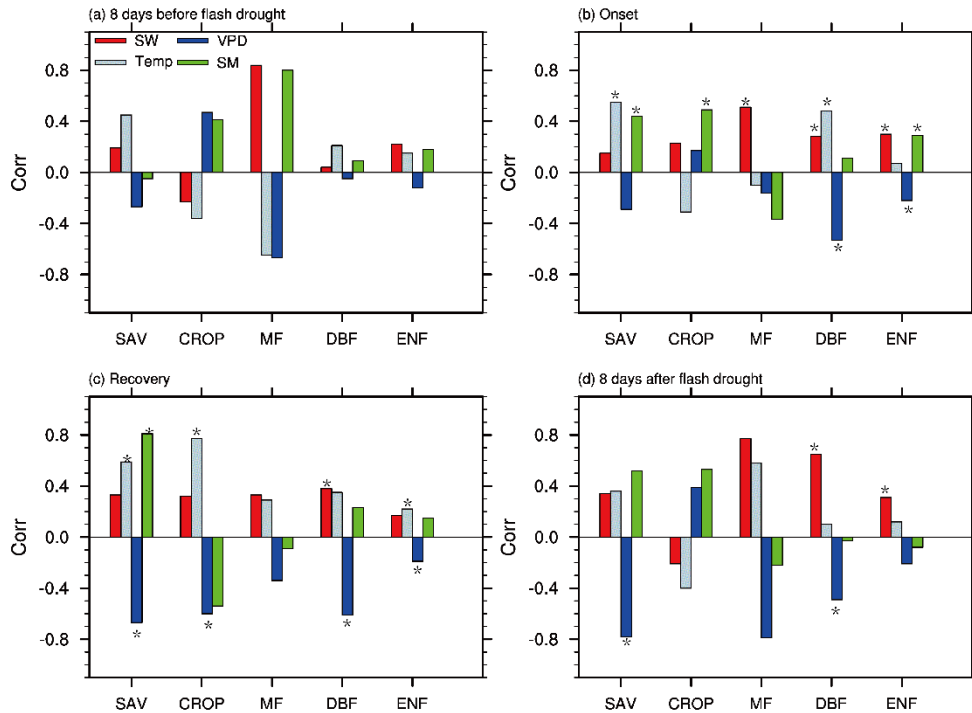
837

838 **Figure 6.** The temporal change rates of standardized GPP anomalies (a-e) and soil
 839 moisture percentiles (f-j) for different vegetation types. SAV: savanna, CROP: rainfed
 840 cropland, MF: mixed forest, DBF: deciduous broadleaf forest and ENF: evergreen
 841 needleleaf forest.



842

843 **Figure 7.** Standardized anomalies of water use efficiency (WUE), underlying WUE
 844 (uWUE), GPP, ET and ET/\sqrt{VPD} during 8 days before flash drought onset, onset
 845 and recovery stages of flash drought events, and 8 days after flash drought.



846

847 **Figure 8.** The partial correlation coefficients between GPP and soil moisture (SM),
 848 shortwave radiation (SW), temperature (Temp) and vapor pressure deficit (VPD) for
 849 different vegetation types including savannas (SAV), rain-fed croplands (CROP),
 850 mixed forests (MF), deciduous broadleaf forests (DBF), and evergreen needleleaf
 851 forests (ENF) during 8 days before soil moisture flash drought, onset and recovery
 852 stages and 8 days after soil moisture flash drought. * indicates the correlation is
 853 statistically significant at the 95% level.

854 **Table 1.** Locations, vegetation types and data periods of Flux Tower Sites used in this
855 study. WSA: woody savanna; CROP: cropland; EBF: evergreen broadleaf forests; MF:
856 mixed forest; DBF: deciduous broadleaf forest; ENF: evergreen needleleaf forest;
857 GRA: grassland; SAV: savanna.

station	lat	lon	IGBP	period
AU-How	-12.49	131.15	WSA	2002-2014
BE-Lon	50.55	4.75	CROP-rainfed	2004-2014
BE-Vie	50.31	6.00	MF	1997-2014
CA-Gro	48.22	-82.16	MF	2004-2013
CA-Oas	53.63	-106.20	DBF	1996-2010
CA-Obs	53.99	-105.12	ENF	1999-2010
CA-TP1	42.66	-80.56	ENF	2002-2014
CA-TP3	42.71	-80.35	ENF	2002-2014
CA-TP4	42.71	-80.36	ENF	2002-2014
CH-Lae	47.48	8.37	MF	2005-2014
CH-Oe2	47.29	7.73	CROP-rainfed	2004-2014
DE-Geb	51.10	10.91	CROP-rainfed	2001-2014
DE-Hai	51.08	10.45	DBF	2000-2012
DE-Kli	50.89	13.52	CROP-rainfed	2005-2014
DE-Tha	50.96	13.57	ENF	1997-2014
FI-Hyy	61.85	24.29	ENF	1997-2014
FI-Sod	67.36	26.64	ENF	2001-2014
IT-Bci	40.52	14.96	CROP-irrigated	2005-2014
IT-Col	41.85	13.59	DBF	2005-2014
IT-Sro	43.73	10.28	ENF	2000-2012
NL-Loo	52.17	5.74	ENF	1999-2013
US-ARM	36.61	-97.49	CROP-rainfed	2003-2013
US-Blo	38.90	-120.63	ENF	1998-2007
US-Me2	44.45	-121.56	ENF	2002-2014
US-MMS	39.32	-86.41	DBF	1999-2014
US-NR1	40.03	-105.55	ENF	2002-2014
US-SRM	31.82	-110.87	WSA	2004-2014
US-UMB	45.56	-84.71	DBF	2002-2014
ZA-Kru	-25.02	31.50	SAV	2000-2010